DOI: 10.1002/chem.200601498

# Intramolecular Excimer Formation and Delayed Fluorescence in Sterically Constrained Pyrene Dimers

**Andrew C. Benniston,* Anthony Harriman,* Sarah L. Howell, Craig A. Sams, and Yong-Gang Zhi[a]**

**Abstract:** The synthesis is described for a series of five molecular dyads comprising pyrene-based terminals covalently linked through a 1,3-disubstituted phenylene spacer. The extent of through-space communication between the pyrene units is modulated by steric interactions imposed by bulky moieties attached at the 6,8-positions of each pyrene unit. For the control compound, only hydrogen atoms occupy the 6,8 positions (**DP1**), whereas the remaining compounds incorporate ethynylene groups terminated with either triisopropylsilyl (**DP2**), 1-*tert*-butylbenzene (**DP3**), 2,6-di-*tert*-butylbenzene (**DP4**) or 1-*tert*-butyl-3,5-dimethylbenzene (**DP5**) units. Each compound shows a mixture of monomer and excimer fluorescence in fluid solution at room temperature, but only monomer emission in a glassy matrix at 77 K. The ratio of monomer to excimer fluorescence depends markedly on the molecular structure; **DP1** is heavily biased in favour of the excimer and **DP4** is enriched with monomer fluorescence. Photophysical properties, including laser induced and delayed fluorescence data, are reported for each compound. Delayed fluorescence occurs by both intramolecular and bimolecular steps, but these events take place on different timescales. The possibility is raised for using intramolecular triplet–triplet annihilation as a means of molecular imaging.

**Keywords:** excimers · fluorescence · imaging agents · pyrene · steric hindrance

## Introduction

π Stacking is an integral part of supramolecular chemistry[1] and provides an invaluable means by which to induce self-association of aromatic subunits, planar heterocycles and unsaturated groups.[2] Double-stranded DNA, including the phenomenon of intercalation, provides the most readily recognised example of π stacking; indeed, such interactions play key roles in protein folding.[3] It is also recognised that π stacking is a major feature of many crystal structures, including certain enzymes. The mutual orientation of the stacking units is of crucial importance in determining the stability of the self-assembled entity, and the two most common arrangements, are "face-to-face" and "edge-to-face" geometries.[4] In the face-to-face orientation, the two units are usually layered in a staggered fashion so as to lower repulsive intermolecular forces,[5] whereas the T-shaped, edge-to-face orientation is particularly abundant in the stacking of protein sidechains.[6] A common feature of all π-stacking interactions is the close proximity of the reactants. The onset of π stacking can be explored by using NMR spectroscopy,[7] while quantum chemical calculations also provide important insight into the binding motif.[8] It is rare for π stacking to be the only form of intermolecular association, and is often found in conjunction with solvophobicity, charge-transfer effects, hydrogen bonding and/or coordinative bonding. Delineating the actual effects of π stacking can be a difficult problem. With the growing interest in molecular electronics, and the understanding that π stacks form good conduits for electronic charge,[9–11] the significance of π stacking seems certain to increase.

Excimer fluorescence forms the basis of many analytical probes[12–15] and can also be used to monitor close interactions between aromatic units. The most popular fluorophore is pyrene,[16] and innumerable examples of inter- and intramolecular excimer formation involving pyrene residues have been reported.[17] The main advantage of this method over NMR spectroscopy is that very low solute concentrations can be used, hence favouring intramolecular association.

[a] Dr. A. C. Benniston, Prof. A. Harriman, Dr. S. L. Howell, Dr. C. A. Sams, Dr. Y.-G. Zhi
Molecular Photonics Laboratory
School of Natural Sciences (Chemistry), Newcastle University
Newcastle upon Tyne, NE1 7RU (UK)
Fax: (+44) 191-222-6929
E-mail: anthony.harriman@ncl.ac.uk

Supporting information for this article is available on the WWW under http://www.chemeurj.org/ or from the author.

   

Excimer fluorescence appears if an excited-state molecule associates with a ground-state molecule. The photon is then delocalised over the conjugate to show a net change in fluorescence spectral profile and lifetime.[16] The resultant photophysical properties can be used to derive structural information about the conjugate and, in turn, can lead to an improved understanding of π-stacking interactions. In particular, intramolecular excimer fluorescence is a strong indicator of the spatial proximity of the relevant subunits given that such emission occurs solely from folded rotamers. Here, we examine the role of bulky blocking groups as a means to control the self-association of pyrene units linked by 1,3-disubstituted benzene spacers. The intention is to balance the π-stacking tendency of the aromatic units, as evidenced by excimer fluorescence, against the inhibitory effects of the side chains. Such studies form an essential part of the protein-folding problem[18] and might lead to the design of next-generation foldamers[19] that possess predetermined electronic properties. With respect to these properties, it is well known[16] that pyrene displays delayed fluorescence by way of triplet–triplet annihilation. A key feature of such P-type delayed fluorescence is that the emission lifetime is unusually long and is set by the timescale for diffusive encounters between pyrene molecules in the triplet state. This could form the basis of an advanced type of fluorescence imaging[20] as the slow decay could be used to discriminate this emission from scattered excitation light and background fluorescence. As such, an integral part of this research programme is to evaluate the sterically congested pyrene dimers and their ability to undergo intramolecular triplet–triplet annihilation on a relatively slow timescale.

## Results and Discussion

**Synthesis**: Pyrene is used extensively in the field of chemical sensors[21] and exhibits an intense structured fluorescence profile in the visible spectral region ($\lambda_{max} = 400$ nm) and a fluorescence lifetime of around 120 ns.[16] In fluid solution, at modest concentrations, the interaction of two pyrene units to form a face-to-face dimer accounts for the observed excimer emission centred at $\lambda \approx 485$ nm. Our devised strategy to control excimer formation involves attaching bulky groups to the 6,8-positions of each pyrene nucleus (Scheme 1). The control dyad, **DP1**, contains no sterically demanding groups and was used as a reference for intramolecular excimer emission.

The starting point for the synthesis was pyrene-2-carboxylic acid **1**, which is readily prepared in a pure form (Scheme 1). This material was converted to the corresponding ester, **2**, by heating the reaction at reflux for 24 h in methanol containing concentrated $H_2SO_4$. Ester **2** was reduced to the corresponding alcohol, **3**, by using $LiAlH_4$ in diethyl ether. Deprotonation of **3** with NaH in dry tetrahydrofuran (THF), followed by reaction with α,α′-dibromo-*m*-xylene, gave the reference compound, **DP1**, in a respectable 95% yield after workup and purification.

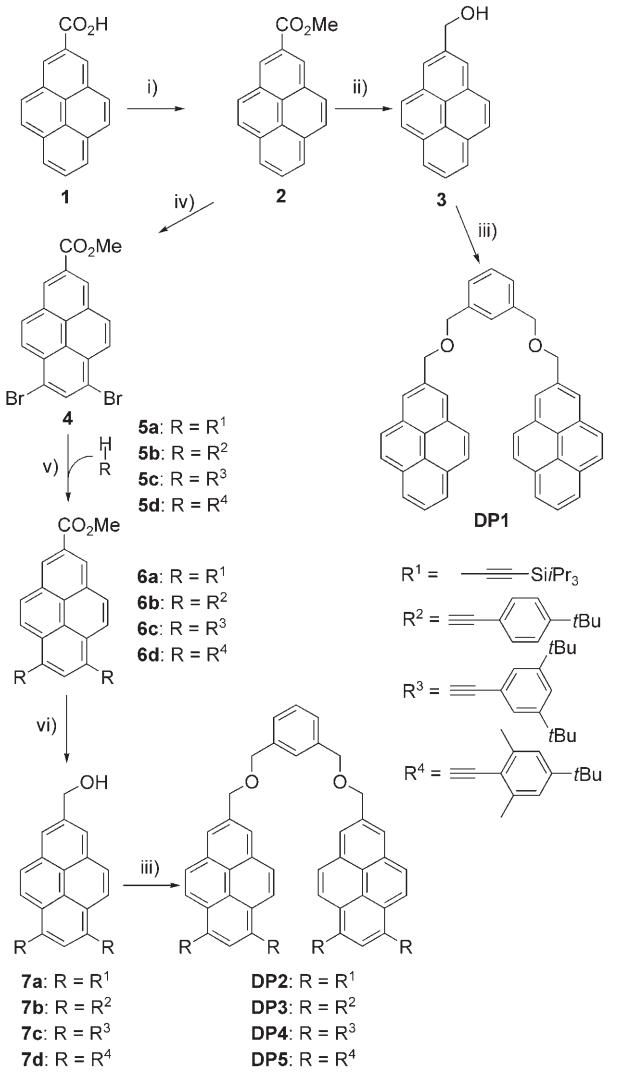


Scheme 1. i) MeOH, $H_2SO_4$ reflux, 24 h; ii) $LiAlH_4$, $Et_2O$, reflux 2 h; iii) NaH, THF, 60 °C; α,α′-dibromo-*m*-xylene, reflux, 12 h; iv) $Br_2$, nitrobenzene, 60 °C; v) $[PdCl_2(PPh_3)_2]$, CuI, THF, $Et_3N$, 55 °C, 24 h; vi) $LiAlH_4$, $Et_2O$, 25 °C, 1 h.

Inspection of a molecular model of **DP1** suggests that incorporation of bulky substituents at the 6,8-positions should hinder face-to-face interactions between the pyrene units. Selective bromination of **2** using $Br_2$ in nitrobenzene afforded the appropriately functionalised pyrene derivative **4** in 96% yield. This compound was used as the main building block for attachment of acetylene-based bulky groups **6a**–**6d** by using standard cross-coupling procedures. Selective reduction of the ester group within **6a**–**6d** using $LiAlH_4$ afforded the desired alcohols, **7a**–**7d**, in good yields. Using the same procedure as for the synthesis of **DP1**, alcohols **7a**–**7d** were reacted with α,α′-dibromo-*m*-xylene to afford dyads **DP2**–**DP5**. These new compounds were fully characterised by means of NMR spectroscopy, mass spectrometry and elemental analysis. All of the compounds are reasonably soluble in most organic solvents at ambient temperature.

  

**Photophysical properties of the reference compound DP1**: The absorption spectrum recorded for the reference system, **DP1**, in cyclohexane is as expected for a non-interacting pyrene dimer.[16] In particular, the lowest energy absorption bands appear as a vibrational progression stretching from $\lambda = 340$ to 300 nm, but on closer inspection the 0,0 transition corresponds to a very weak band at 365 nm (Figure 1). Observation of this latter band is important because it indicates that the lowest-energy, singlet-excited state ($S_1$) has $^1L_b$ character. As such, we would expect a modest fluorescence quantum yield but a long fluorescence lifetime.[22] The absorption spectrum is insensitive to changes in solute concentration or solvent polarity. Fluorescence spectra recorded for dilute solutions of **DP1** show two regions of interest. There is a set of partially resolved bands across the $\lambda = 360$–410 nm region but the spectrum is dominated by a featureless band centred at 485 nm (Figure 1). Based on earlier work with simpler pyrene derivatives,[23] the higher-energy bands can be assigned to monomer (i.e., $S_1$) fluorescence, whereas the lower-energy band can be attributed to an excimer. The total fluorescence quantum yield ($\Phi_F$) measured in deoxygenated cyclohexane at 20 °C is 0.25 (Table 1); the ratio of integrated monomer (M) and excimer (E) fluorescence spectral profiles resolved from the steady-state spectrum ($S_{M/E}$) is 25-fold in favour of the excimer. The same situation is found for **DP1** in both ethanol and acetonitrile. Progressively diluting the sample up to a factor of $10^4$ has no observable effect on the spectral profile and, in particular, does not shift the balance towards monomer emission. This finding confirms that the excimer arises from intramolecular association of two pyrene units and is, therefore, a folded rotamer. In a frozen ethanol glass at 77 K, however, only monomer fluorescence is observed (Figure 1). This situation is consistent with excimer formation taking place after excitation, as opposed to illumination of a ground-state dimer. In all cases, the corrected excitation spectrum gave a good match to the absorption spectrum.

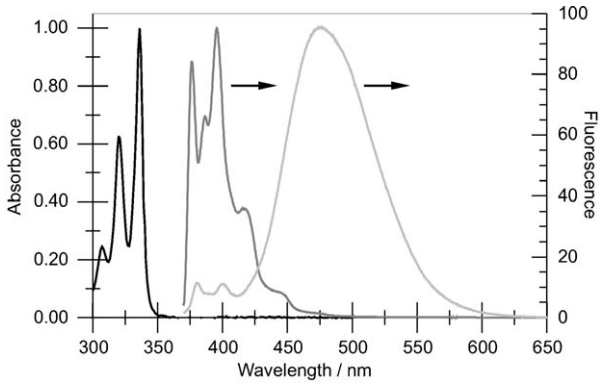


Figure 1. Absorption (black) and fluorescence (light grey) spectra recorded for **DP1** in cyclohexane at RT and the fluorescence spectrum (dark grey) recorded in a glassy ethanol matrix at 77 K.

Table 1. Photophysical properties recorded for the various pyrene dimers in deoxygenated cyclohexane at 20 °C.

| Property | DP1 | DP2 | DP3 | DP4 | DP5 |
|---|---|---|---|---|---|
| $\Phi_F$ | 0.25 | 0.78 | 0.38 | 0.88 | 0.65 |
| $\tau_{M1}$ [ns] | 3.5 | 4.4 | 2.1 | 6.3 | 3.4 |
| $\tau_{M2}$ [ns] | 45 | 43 | 30 | 17 | 28 |
| $S_{M/E}$ | 0.04 | 2.5 | 1.9 | 7.0 | 1.8 |
| $\tau_T$ [μs] | 100 | 110 | 95 | 90 | 95 |
| $\tau_{ION}$ [μs] | – | 1.9 | 2.0 | 2.1 | 2.0 |
| $\Phi_{DF}$ | – | 1.00 | 0.42 | 0.34 | 0.40 |
| $\tau_{DF}$ [ns] | – | 55 | 33 | 120 | 45 |

In deoxygenated cyclohexane, fluorescence from pyrene decays by means of single exponential kinetics with a lifetime of $\approx 120$ ns but more complex behaviour was found for **DP1** under the same conditions (Table 1). Examination of the monomer emission at $\lambda \approx 380$ nm shows that fluorescence decay profiles, $I_F(t)$, can be satisfactorily described as the sum of two exponential components, according to Equation (1) (Figure 2). Here, $A$ refers to the fractional amplitude of a particular component with a lifetime $\tau$; under these conditions, $A_1/A_2 \approx 17$. Increasing the number of exponential terms did not improve the quality of the fit as judged by the usual statistical criteria.[24] This is perhaps due to the phenylene spacer restricting the range of available conformations. Monitoring the excimer fluorescence at $\lambda = 470$ nm also requires analysis of dual-exponential kinetics, in line with Equation (2) (Figure 2). In this case, the signal grows-in after the excitation pulse before decaying. Within the margin of experimental error, $\tau_{M1} = \tau_{E1}$ and $\tau_{M2} = \tau_{E2}$. Slightly different lifetimes were obtained in other solvents, but the basic behaviour remained as described above.

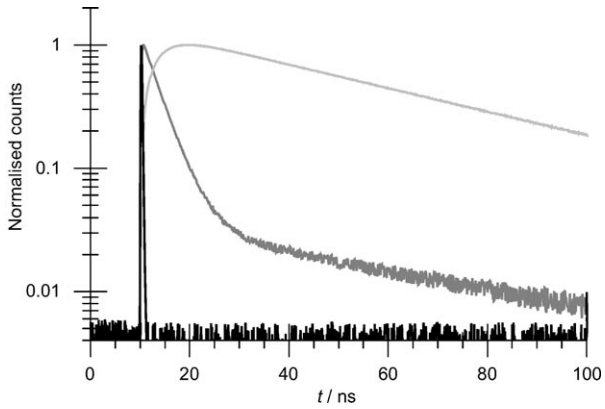


Figure 2. Fluorescence decay profiles recorded by time-correlated, single-photon counting for **DP1** in deoxygenated cyclohexane at RT, showing emission for the monomer (dark grey), excimer (light grey) and the instrumental response function (black).

$$I_F^M(t) = A_1 \exp\left(-\frac{t}{\tau_{M1}}\right) + A_2 \exp\left(-\frac{t}{\tau_{M2}}\right) \quad (1)$$

$$I_F^M(t) = G_2\exp\left(-\frac{t}{\tau_{E2}}\right) + G_1\exp\left(-\frac{t}{\tau_{E1}}\right) \quad (2)$$

Based on the wealth of prior experimental studies pertaining to intramolecular excimer formation,[25] the kinetic data can be explained in terms of Scheme 2. The shorter lifetime

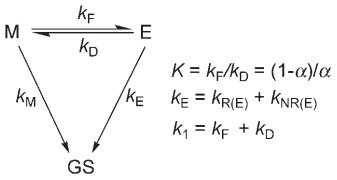


Scheme 2. Proposed pathways for decay of the monomer (M) and excimer (E) to the ground state (GS). The derived parameters are listed in Table 2.

($\tau_{M1}$), relative to that recorded for pyrene, reflects the dynamics of the diffusional processes needed for self-association. This process is reversible and rate constants for the formation ($k_F$) and dissociation ($k_D$) of the excimer can be extracted from the time-resolved fluorescence data. The longer lifetime ($\tau_{M2}$) refers to the decay of the equilibrated mixture of monomer and excimer, and can be used to derive the rate constants for the inherent decay of the monomer ($k_M$) and excimer ($k_E$). These latter processes comprise both radiative and non-radiative events. The radiative rate constant for excimer emission ($k_{R(E)}$) was calculated by iterative reconstitution of the steady-state spectrum. The derived values are compiled in Table 2. Notably, triplet formation is inefficient for **DP1**, although the triplet lifetime ($\tau_T$) is quite long in deoxygenated cyclohexane (Table 1). Despite the apparent simplicity of Scheme 2, and the assumptions that underlie it, several useful conclusions can be derived that could be instructive in understanding the other systems. Firstly, formation of the excimer ($k_F$) is reasonably fast but reversible dissociation ($k_D$) is slow. Secondly, on the assumption that $k_M$ can be equated to that for pyrene ($k_M = 8.3\times 10^6\ s^{-1}$), the excimer decays almost exclusively by routes that do not involve repopulation of the monomer excited state.

Table 2. Kinetic and thermodynamic properties derived for the various pyrene dimers in deoxygenated cyclohexane on the basis of Scheme 2.

| Property | DP1 | DP2 | DP3 | DP4 | DP5 |
|---|---|---|---|---|---|
| $k_1\times10^8$ [$s^{-1}$] | 2.9 | 1.0 | 3.5 | 0.34 | 1.70 |
| $k_F\times10^8$ [$s^{-1}$] | 2.7 | 0.96 | 3.44 | 0.27 | 1.62 |
| $k_D\times10^7$ [$s^{-1}$] | 0.2 | 0.60 | 0.70 | 0.70 | 0.80 |
| $A_1$ [%] | 97.2 | 88.9 | 94.7 | 76.9 | 90.9 |
| $K$ | 17 | 15.7 | 49 | 3.8 | 20 |
| $k_M\times10^7$ [$s^{-1}$] | 0.83 | 12.5 | 12.5 | 12.5 | 12.5 |
| $k_E\times10^7$ [$s^{-1}$] | 2.4 | 1.7 | 3.2 | 4.1 | 3.1 |
| $\alpha$ | 0.06 | 0.06 | 0.02 | 0.21 | 0.05 |
| $k_{R(E)}\times10^7$ [$s^{-1}$] | 0.04 | 1.2 | 1.1 | 1.5 | 1.4 |
| $k_{NR(E)}\times10^7$ [$s^{-1}$] | – | 0.5 | 2.5 | 2.6 | 1.7 |

**Photophysical properties of DP2–DP5**: The presence of alkynylene substituents on the pyrene units induces a significant redshift for the lowest-energy absorption bands (Figure 3), although the spectral profile remains similar to

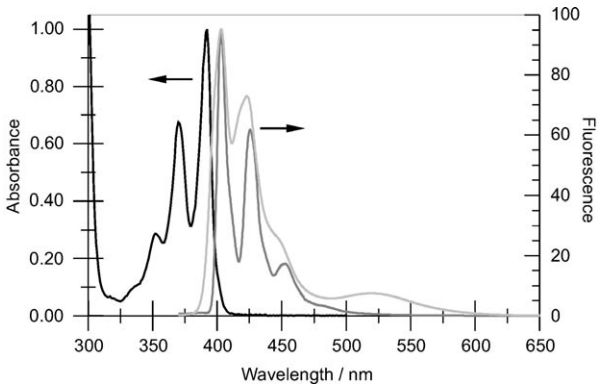


Figure 3. Absorption (black) and fluorescence (light grey) spectra recorded for **DP2** in cyclohexane at RT and the fluorescence spectrum (dark grey) recorded in a glassy ethanol matrix at 77 K.

that of **DP1**. For these compounds, the $S_1$ state has $^1L_a$ character; typical properties being fluorescence quantum yields approaching unity, but relatively short fluorescence lifetimes.[22] The position of the 0,0 transition ($\lambda_{00}$) varies slightly among the compounds (Table 3), which must be due to a weak electronic effect associated with the substitution pattern. This behaviour indicates a rather subtle effect imposed by the substituent. The fluorescence spectrum shows a mixture of monomer and excimer bands (Figures 3 and 4), with both fluorescence and absorption spectra being redshifted with respect to **DP1**. Electronic effects also affect the maxima of the monomer ($\lambda_M$) and excimer ($\lambda_E$) fluorescence peaks. The absence of any spectral changes upon serial dilution confirms that excimer fluorescence is the result of intramolecular associations between the pyrene units, in both cyclohexane and ethanol at ambient temperature. At 77 K, however, only monomer fluorescence is observed (Figure 3). Corrected excitation spectra were found to agree with the corresponding absorption spectra across the near UV region. The energy difference between the respective maxima of monomer and excimer emission bands provides a crude measure of the free energy of stabilisation ($\Delta G_{GS}$) of

Table 3. Spectroscopic properties recorded for the various pyrene dimers in cyclohexane, together with the molar volumes of the substituent groups.

| Cmpd | $\lambda_{00}$ [nm] | $\lambda_M$ [nm] | $\lambda_E$ [nm] | $\Delta G_{GS}$ [kJ mol$^{-1}$] | $V_{MOL}$ [b] |
|---|---|---|---|---|---|
| **DP1** | 337[a] | 377 | 471 | 63.3 | – |
| **DP2** | 392 | 395 | 523 | 74.1 | 125.8 |
| **DP3** | 410 | 422 | 525 | 55.6 | 90.2 |
| **DP4** | 403 | 420 | 514 | 52.1 | 134.5 |
| **DP5** | 414 | 427 | 532 | 55.3 | 117.5 |

[a] Refers to the first intense absorption transition. [b] Molar volume of the substituent in units of cm$^3$mol$^{-1}$.

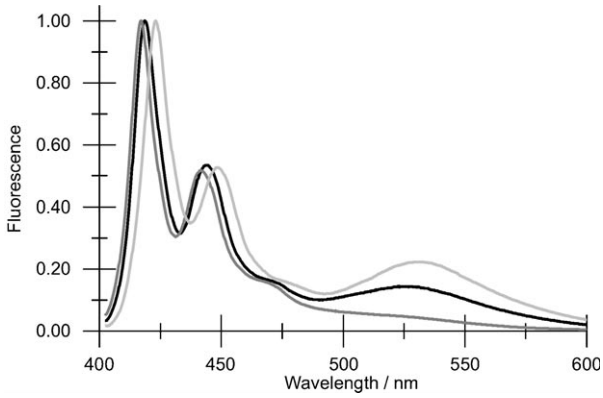


Figure 4. Comparison of the fluorescence spectra recorded for **DP3** (black), **DP4** (dark grey) and **DP5** (light grey) in deoxygenated cyclohexane at RT.

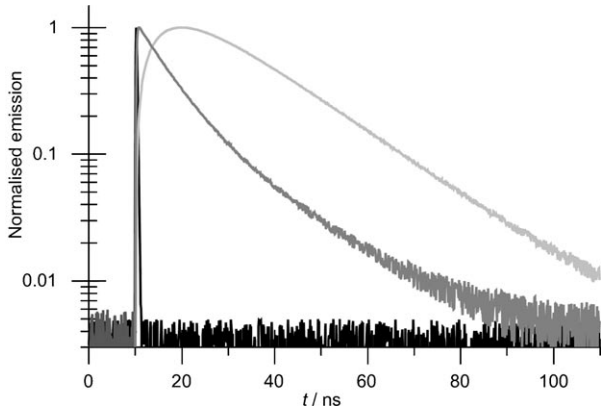


Figure 5. Fluorescence decay profiles recorded by time-correlated, single-photon counting for **DP4** in deoxygenated cyclohexane at RT, showing emission for the monomer (dark grey), excimer (light grey) and the instrumental response function (black).

the excimer (Table 3). The derived values for **DP3**–**DP5** are comparable, as might be expected on the basis of their similar structures. These excimers are subject to far less stabilisation than **DP1**, in which the pyrene nuclei can come into closer contact. However, **DP2** shows a considerably higher level of stabilisation. In each case the ratio ($S_{M/E}$) of the quantum yields for monomer and excimer fluorescence in the steady-state spectrum is considerably higher than that for **DP1**. Indeed, there is a surprisingly large variation in $S_{M/E}$ that does not appear to be related to the size of the blocking group, as illustrated by the relative molar volume ($V_{MOL}$)[26] (Table 1). We note that **DP4** shows little tendency to form an excimer.

The photophysical properties derived for the pyrene dimers in deoxygenated cyclohexane are listed in Table 1. The overall fluorescence quantum yields ($\Phi_F$) vary somewhat throughout the series but remain high due, at least in part, to the high radiative rate constants inherent to ethynylated pyrene fluorophores.[27] In each case, fluorescence from the monomer decays through dual-exponential kinetics, in accordance with Equation (1), and the two lifetimes, $\tau_{M1}$ and $\tau_{M2}$, are given in Table 1. Fluorescence from the excimer grows-in with a lifetime comparable to $\tau_{M1}$ before decaying with a lifetime similar to $\tau_{M2}$ (Figure 5). At wavelengths at which only monomer fluorescence is detected, the fractional contribution of the shorter-lived species ($A_1$) greatly exceeds that ($A_2 = 1 - A_1$) of the longer-lived species (Table 2). However, because $\tau_M$ (8.2 ns) is in the range expected for an ethynylated pyrene-based $^1L_a$ state ($4 < \tau < 10$ ns),[27] it cannot be assumed that $\tau_M$ relates to the time taken to establish the equilibrium between monomer and excimer species. Indeed, time-gated fluorescence spectra show that $S_{M/E}$ decreases steadily with time over the first few nanoseconds until reaching a constant value.

Transient differential absorption spectra were recorded following laser excitation ($\lambda = 355$ nm; full width at half maximum (fwhm) = 4 ns) of solutions of the pyrene dimers in deoxygenated cyclohexane. The derived spectra show certain common features (Figure 6). Consequently, ground-state bleaching can be observed at $\lambda < 400$ nm in addition to pronounced absorption in the range 400–600 nm. At modest laser powers, the signal decays by complex kinetics that can be approximated as the sum of two exponential components. The shorter-lived species has a lifetime of $\approx 2$ μs in each case. The longer-lived transient corresponds to a lifetime ($t_T$) of $\approx 100$ μs in the absence of oxygen (Table 1). Addition of oxygen quenches the entire signal but, in the presence of iodoethane (10% v/v) the yield of the longer-lived species is increased, while the shorter-lived species decreases in significance. At very low laser power, only the longer-lived species is observed. On this basis, the longer-lived transient can be assigned to the pyrene-based triplet excited state.[28]

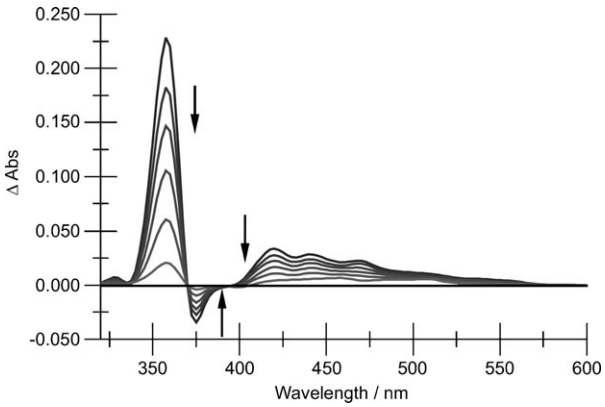


Figure 6. Differential triplet–triplet absorption spectra recorded after laser flash excitation of a solution of **DP4** in deoxygenated cyclohexane.

The shorter-lived component ($\tau_{ION}$), which exhibits a different spectrum to the triplet state (Figure 6), is observed only at relatively high laser power and must, therefore, be a consequence of a multi-photon effect. A probable assignment for this species is the pyrene π-radical cation formed by photo-ionisation,[29] but this possibility was not explored in detail. In the event that the shorter-lived species is the result of two-photon ionisation, the second photon must be

  

absorbed by the excimer as identical behaviour is found for **DP1**. The net result of these various processes is to minimise the yield of the triplet excited state.

The time-resolved fluorescence data were analysed according to Scheme 2 to expose the individual rate constants (see the Supporting Information for a detailed description of the methodology used for data analysis) and the main results are collected in Table 2. Here, $k_1$ refers to the rate constant for fluorescence quenching, whereas $k_F$ and $k_D$, respectively, refer to the rate constants for the formation and reversible dissociation of the excimer. These last two values can be used to calculate the equilibrium constant, $K$, for the excimer and the fraction of monomer, $\alpha$, present in the equilibrium mixture. It is apparent that $k_F$ decreases linearly with increasing molar volume of the substituent (see the Supporting Information). Given that $k_D$ is essentially independent of $V_{MOL}$, it follows that both $K$ and $\alpha$ are sensitive to the volume of the substituent. These effects are probably associated with changes in the diffusion coefficients of the pyrene units and/or the frequency with which suitable geometries are reached upon collision between units. Across the series, there is a 13-fold variation in $k_F$, and the results indicate that the inefficient excimer formation noted for **DP4** arises because of the bulky substituent. The excimer decays by way of thermal repopulation of $S_1$, thereby giving rise to delayed fluorescence, in addition to radiative ($k_{R(E)}$) and non-radiative ($k_{NR(E)}$) pathways. The derived $k_{R(E)}$ values tend toward an average value of $1.3\times10^7\ s^{-1}$ but the corresponding $k_{NR(E)}$ values show a crude linear correlation with $\Delta G_{GS}$ (see Supporting Information). This latter trend serves to control the fluorescence yield and lifetime for the excimer and it is notable that **DP2** forms the most fluorescent excimer.

**Triplet–triplet annihilation**: The triplet yield can be increased dramatically by addition of iodoethane (10% v/v), although the triplet lifetime is shortened to around 10 μs by the external heavy-atom effect.[30] Under these conditions, delayed fluorescence can be observed following exposure to intense laser pulses ($\lambda=355$ nm; fwhm = 4 ns) in deoxygenated cyclohexane (Figure 7).[31] The resultant spectral profile is similar to that of the equilibrium mixture of the monomer and excimer.[32] The yield increases with increasing laser power and corresponds to a two-photon process (see the Supporting Information). Under the same conditions, transient absorption spectra show that the triplet state undergoes triplet–triplet annihilation (TTA).[33] Therefore, the source of the delayed fluorescence can be traced to the interaction between two triplet states according to Scheme 3.

Decay of the delayed fluorescence involves biphasic kinetics in each case, although the spectral profile does not change with time (Figure 8). The longer-lived component, which makes a relatively minor contribution to the total signal, has a half-life of ≈5 μs at the highest available laser power but this value depends on the initial triplet concentration. The latter can be varied by dilution or by modulation of the laser power. Systematic changes in triplet concentration indicate that the longer-lived component is the result of a bimolecular process and that the rate constant for diffusional encounter of two triplet states ($k_{TTA}$) is $\approx1\times10^9\ M^{-1}s^{-1}$ in deoxygenated cyclohexane at 20 °C. This is well below the diffusion-controlled rate limit, suggesting that many encounters are needed before the appropriate geometry is found. The kinetics of intermolecular triplet–triplet annihilation have been considered in terms of spin-re-

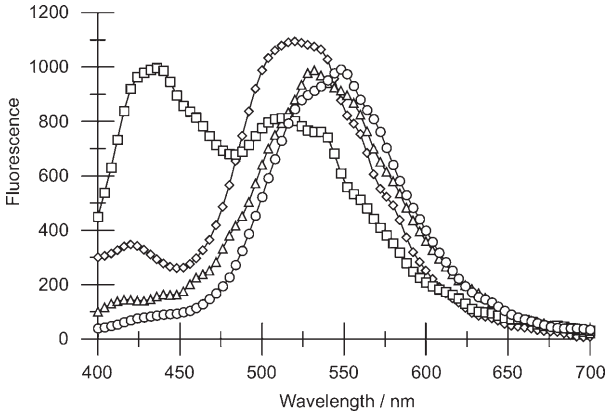


Figure 7. Delayed fluorescence spectra recorded at high laser intensity in deoxygenated cyclohexane containing 10% v/v iodoethane; **DP2** (◇), **DP3** (△), **DP4** (□), **DP5** (○).

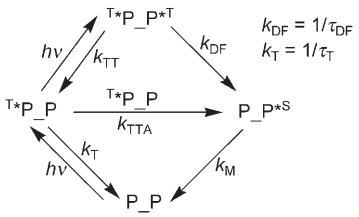


Scheme 3. Proposed routes leading to triplet–triplet annihilation and subsequent intramolecular and intermolecular delayed fluorescence.

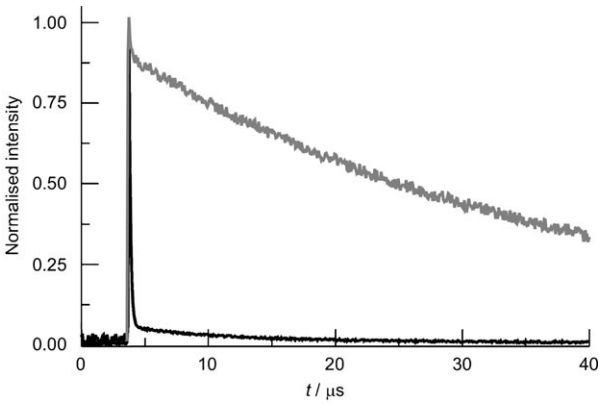


Figure 8. Decay profiles recorded for the delayed fluorescence observed with **DP4** in deoxygenated cyclohexane using a high laser intensity at concentrations of 2 μM (dark grey) and 50 μM (black). Note, the signals have been normalised for clarity of presentation.

  

striction rules and the mechanism for such delayed fluorescence has been resolved,[34] including the observation of both monomer and excimer emission.[35] We can consider that these pyrene dimers behave similarly in terms of their bimolecular interactions. Identical results were obtained for each compound within the series **DP2–DP5**. However, it was not possible to make meaningful measurements for **DP1** because of the poor absorption profile around the available laser-excitation wavelengths.

The shorter-lived component could be approximated to first-order kinetics and the derived lifetimes ($\tau_{DF}$) are compiled in Table 1. There is considerable variation among the series, in which **DP4** displays a particularly long lifetime for the delayed fluorescence. In contrast, **DP2** and **DP3** show $\tau_{DF}$ values close to those found for excimer emission. These lifetimes are independent of the initial triplet concentration and clearly correspond to a unimolecular process. There is a good correlation between $k_F$, the rate constant for formation of the excimer, and the inverse of $\tau_{DF}$ (see Supporting Information). The gradient of the resultant linear plot is $\approx 0.3$, indicating that TTA is subject to more restrictions than is excimer formation. Prior work[34,35] has established that the rate of bimolecular TTA is slower than the diffusion-controlled rate limit, in which the fractional reduction is dependent on both the solvent and solute. Such behaviour is consistent with spin-restriction rules.

For the compounds considered here the majority of the detected delayed fluorescence arises from the unimolecular pathway, although it should be realised that intramolecular TTA involves processes other than delayed fluorescence, such as that denoted by $k_{TT}$ in Scheme 3. The relative quantum yields for delayed fluorescence ($\Phi_{DF}$) also vary throughout the series (Table 1) but can be well explained in terms of the $k_{R(E)}$ and $k_{NR(E)}$ values derived earlier. Therefore, **DP2** gives the highest yield of delayed fluorescence under standardised conditions and this compound is characterised by a relatively low $k_{NR(E)}$ value. Furthermore, **DP4** shows a much higher $k_{NR(E)}$ value and a correspondingly low yield of delayed fluorescence. It should be noted that spin-restriction rules lower the rate constant for direct formation of an excited singlet state by means of TTA to around one-ninth of the diffusion-controlled limit.[34,35]

**Role of the blocking groups**: Seemingly minor variations in the nature of the blocking groups cause serious perturbation of the photophysical properties of both the monomer and excimer and also affect the yield and lifetime of the delayed fluorescence. Excimer formation is observed in each case but the steady-state yields vary considerably throughout the series. This effect can be traced to variations in $k_F$ and there is a direct correlation between $k_F$ and the molar volume of the blocking group (see the Supporting Information). Indeed, $k_F$ varies by a factor of 13 among the series. This simple relationship is a clear testimony of the need for the pyrene units to form a $\pi$ stack to stabilise the excimer. As a consequence of the steric effect on $k_F$, there is a corresponding modulation of $K$ and, more importantly, the fractional contribution ($\alpha$) of monomer present at equilibrium. This latter term influences the fluorescence spectral profile, particularly the delayed fluorescence, and makes an important contribution towards the lifetime of the excimer. Finally, the role of the ethynylene groups should not be overlooked given that these cause inversion of the $^1L_a$ and $^1L_b$ excited states and thereby impose high radiative rate constants. These rate constants are carried through to the excimer and there is a surprising consistency in the derived $k_{R(E)}$ values (Table 2). However, the lifetime of the excimer is controlled by a combination of reverse population of the $S_1$ state and non-radiative decay. Whereas $k_D$ depends weakly on the nature of the substituent, there is a more profound variation in the derived $k_{NR(E)}$ values, which strongly affects the fluorescence yield of the excimer. It is clear that $k_{NR(E)}$ does not depend on the size of the substituent but does show a linear relationship with $\Delta G_{GS}$.

The reason why **DP2** forms such a stable excimer is unclear; it cannot be a simple effect of stereochemistry, as **DP1** is far less sterically constrained, and must involve an electronic effect. Accordingly, this effect must reflect some property of the silicon atom. Simple molecular-orbital calculations made at the AM1 level indicate that the interposed silicon atom restricts both the HOMO and LUMO to the ethynylated pyrene residues, whereas more extended delocalisation is inherent to the other derivatives. To what effect this influences excimer emission is not obvious at present, but it seems to be a rather fortunate consequence of this type of blocking group that could be exploited in future prototypes.

Intramolecular triplet–triplet annihilation leads to delayed fluorescence that persists for unusually long times.[31,33] There is a clear correlation between $\tau_{DF}$ and $k_F$, such that both parameters are set by steric factors. This finding suggests that TTA requires orbital contact between the polycycles. In each case, the spectral profile recorded for delayed fluorescence corresponds to that characterised by time-gated emission spectra as belonging to the equilibrated mixture. Except for **DP4**, this spectrum is dominated by emission from the excimer. This is a useful property for a fluorescent sensor because it helps to separate excitation and emission wavelengths and thereby minimise contamination by scatter. The temporal profile offered by such delayed fluorescence is a great bonus with respect to avoiding background fluorescence and scattering effects. As such, it will be interesting to evaluate next-generation prototypes as a novel form of fluorescence imaging. Detailed studies are ongoing in our laboratory.

## Experimental Section

**Materials**: All chemicals were purchased from commercial sources and were used as received. Solvents for synthesis were dried by using standard literature methods[36] before being distilled and stored under nitrogen over 4 Å molecular sieves. $^1H$ and $^{13}C$ NMR spectra were recorded by using a JEOL Lambda 500 MHz or Bruker AVANCE 300 MHz spectrometer. Within the NMR data B and P represent Benzene and Pyrene

  

respectively. Routine mass spectra and elemental analyses data were obtained by using in-house facilities. The starting materials pyrene-2-carboxylic acid (**1**),[37] **5b**,[38] **5c**[39] and **5d**[40] were prepared by using literature methods and purified extensively before use.

**Methods**: Absorption spectra were recorded by using a Hitachi U3310 spectrophotometer. All fluorescence studies were carried out by using a Yvon-Jobin fluorolog tau-3 spectrometer. Fluorescence spectra were corrected for spectral imperfections by using a standard lamp. Measurements were made by using optically dilute solutions after that had been deoxygenated by purging with dried $N_2$. Fluorescence quantum yields were measured with respect to 9,10-dimethylanthracene in deoxygenated cyclohexane.[41] Corrected excitation spectra were also recorded under optically dilute conditions. Fluorescence lifetimes were measured by using time-correlated, single-photon counting conditions following excitation by a laser diode at $\lambda = 340$ nm. After deconvolution of the instrument response function, the temporal resolution of our setup was $\approx 100$ ps. Low-temperature studies were carried out by using an immersion-well Dewar filled with liquid $N_2$.

Laser flash photolysis studies were carried out by using an Applied Photophysics LKS 60 instrument. An excitation beam was generated at $\lambda$355 nm by using a frequency-tripled, Nd–YAG laser. The pulse width was $\approx 4$ ns. A high-intensity, pulsed Xe arc lamp was used for the monitoring beam, and was kept perpendicular to the excitation beam. The monitoring beam was passed through a high-radiance monochromator and was detected with a fast response photo multiplying tube (PMT). Transient differential absorption spectra were recorded point-by-point with five separate records being averaged at each wavelength. Kinetic data were obtained by averaging about 100 individual records collected at a particular wavelength. Solutions for flash photolysis were prepared that have an absorbance of $\approx 0.20$ at $\lambda = 355$ nm. All solutions were deoxygenated prior to the experiments by purging with dried $N_2$.

**Preparation of pyrene-2-carboxylic acid methyl ester (2)**: Pyrene-2-carboxylic acid, **1** (0.20 g, 0.81 mmol) was dissolved in MeOH (40 mL) containing concentrated $H_2SO_4$ (1 mL) and was heated at reflux for 24 h. The solution was cooled to RT and the solvent was removed to afford a residue that was redissolved in $CH_2Cl_2$ (80 mL), and then washed with $H_2O$ (30 mL), $Na_2CO_3$ (30 mL) solution and $H_2O$ again. The organic layer was separated, dried over $MgSO_4$, filtered and evaporated. The concentrated residue was purified by means of column chromatography on silica gel by using petroleum ether/ethyl acetate (1:10) as the eluant to afford a white solid (0.21 g, 99%). $^1$H NMR (300 MHz, $CDCl_3$, 25°C): $\delta = 8.80$ (s, 2H; $^1$H, $^3$H), 8.19 (d, $J = 7.4$ Hz, 2H; $^6$H, $^8$H), 8.08 (d, $J = 9.0$ Hz, 2H; $^4$H, $^{10}$H), 8.04 (d, $J = 9.0$ Hz, 2H; $^5$H, $^9$H), 8.04 (dd, $J = 7.2$ Hz, $J' = 7.2$ Hz, 1H; $^7$H), 4.06 ppm (s, 3H; OMe); $^{13}$C NMR (75 MHz, $CDCl_3$, 25°C): $\delta = 167.61$, 131.90, 131.05, 128.14, 127.74, 127.47, 127.02, 126.96, 125.72, 125.39, 124.45, 52.23 ppm; EI-MS: $m/z$: calcd for $C_{18}H_{12}O_2$: 260; found: 260 $[M]^+$, 229 ,$[M-OCH_3]^+$.

**Preparation of pyren-2-yl-methanol (3)**: $LiAlH_4$ (0.4 g, 11.8 mmol) was suspended in dry $Et_2O$ (150 mL) in a three-neck flask under a dry nitrogen atmosphere. Ester **2** (2.1 g, 8.07 mmol) was then added as a solid. After addition, the mixture was stirred for 3 h, and heated at reflux for a further 2 h, cooled to RT, and poured carefully into ethyl acetate. A few drops of $H_2O$ were added carefully, followed by a larger addition $H_2O$ (50 mL). The aqueous phase was extracted with ethyl acetate (3×80 mL). The combined organic phase was dried over $MgSO_4$, filtered and evaporated to afford a residue that was purified by means of column chromatography on silica gel by using ethyl acetate/petroleum ether (1:6) as eluant to give a white solid (1.87 g, 100%). $^1$H NMR (300 MHz, $CDCl_3$, 25°C): $\delta = 8.13$ (d, $J = 7.2$ Hz, 2H; $^6$H, $^8$H), 8.11 (s, 2H; $^1$H, $^3$H), 8.04 (d, $J = 9.0$ Hz, 2H; $^5$H, $^9$H), 8.00 (d, $J = 9.0$ Hz, 2H; $^4$H, $^{10}$H), 7.94 (t, $J = 7.2$ Hz, $J' = 7.2$ Hz, 1H; $^7$H), 5.08 ppm (s, 2H; $OCH_2$); $^{13}$C NMR (75 MHz, $CDCl_3$, 25°C): $\delta = 139.07$, 131.87, 131.56, 128.08, 127.64, 126.19, 125.42, 125.05, 124.69, 123.63, 66.19 ppm; EI-MS: $m/z$: calcd for $C_{17}H_{12}O$: 232; found: 232 $[M]^+$, 215 $[M-OH]^+$.

**Preparation of 6,8-dibromopyrene-2-carboxylic acid methyl ester (4)**: Ester, **2**, (0.22 g, 0.85 mmol) was dissolved in nitrobenzene (10 mL) and heated to 60°C. To this, a solution of bromine (0.22 mL) dissolved in nitrobenzene (2 mL) was added dropwise over 1 h. The solution was stirred at 60°C for a further 4 h, cooled to RT and left to stand overnight. The resultant solid was filtered, washed with cold EtOH, then $Et_2O$ and dried in air to give a pale-yellow solid (0.34 g, 96%). EI-MS: $m/z$: calcd for $C_{18}H_{10}Br_2O_2$: 418; found: 418 $[M]^+$, 387 $[M-OCH_3]^+$, 359 $[M-CO_2CH_3]^+$. (Because of the poor solubility of the compound, no NMR data were collected.)

**Preparation of 6,8-di(isopropylsilylprop-1-ynyl)pyrene-2-carboxylic acid methyl ester (6a)**: Ester **4** (0.42 g, 1.00 mmol), copper(I) iodide (14 mg, 0.074 mmol) and dichlorobis(triphenylphosphine)palladium(II) (77 mg, 0.11 mmol) were combined in a three-neck flask flushed with nitrogen. The solids were dissolved in THF (60 mL) containing $Et_3N$ (20 mL), and the solution thoroughly purged with nitrogen for 1 h. Triisopropylsilyl acetylene **5a** (0.82 mL, 3 mmol) was added dropwise through a syringe to the stirred solution. After the solution had been stirred for 20 min, the temperature of the reaction mixture was raised to 55–60°C and maintained for 24 h. The solvent was removed and the residue was extracted with $CH_2Cl_2$ (120 mL), washed with $H_2O$ (2×30 mL) and dried over $MgSO_4$. Following filtration, the volatile component was removed and the crude material was purified by means of column chromatography on silica gel by using ethyl acetate/petroleum ether (1:8 then 1:2) as the eluant to give a white solid (0.62 g, 99%). $^1$H NMR (300 MHz, $CDCl_3$, 25°C): $\delta = 8.79$ (s, 2H; $^1$H, $^3$H), 8.57 (d, $J = 9.1$ Hz, 2H; $^5$H, $^9$H), 8.25 (s, 1H; $^7$H), 8.18 (d, $J = 9.1$ Hz, 2H; $^4$H, $^{10}$H), 4.03 (s, 3H; OMe), 1.18–1.17 ppm (m, 42H; *i*Pr); $^{13}$C NMR (75 MHz, $CDCl_3$, 25°C): $\delta = 167.62$, 135.21, 133.15, 131.47, 129.64, 128.52, 127.04, 126.67, 126.62, 124.53, 119.00, 105.14, 98.29, 52.67, 19.13, 11.94 ppm; EI-MS: $m/z$: calcd for $C_{40}H_{52}O_2Si_2$: 620; found: 620 $[M]^+$, 589 $[M\text{-}OCH_3]^+$.

**Preparation of [6,8-di(isopropylsilylprop-1-ynyl)pyren-2-yl]-methanol (7a)**: Ester **6a** (1.0 g, 1.6 mmol) was dissolved in dry $Et_2O$ (80 mL) in three-neck flask under a nitrogen atmosphere. $LiAlH_4$ (0.1 g, 2.64 mmol) was added carefully to the stirred solution, and then stirred for a further 1 h. The mixture was added to ethyl acetate (100 mL) containing $H_2O$, to which dilute HCl was added carefully. The organic phase was washed with $H_2O$ (2×30 mL), dried over $MgSO_4$ and evaporated to give a residue that was purified by means of column chromatography on silica gel by using ethyl acetate/petroleum ether (1:3) as the eluant to afford a yellow-green solid (0.94 g, 98%). $^1$H NMR (300 MHz, $CDCl_3$, 25°C): $\delta = 8.53$ (d, $J = 9.0$ Hz, 2H; $^5$H, $^9$H), 8.20 (s, 1H; $^7$H), 8.15 (s, 2H; $^1$H, $^3$H), 8.11 (d, $J = 9.0$ Hz, 2H; $^4$H, $^{10}$H), 5.09 (s, 2H; $OCH_2$), 1.18–1.17 ppm (m, 42H; Si*i*Pr); $^{13}$C NMR (75 MHz, $CDCl_3$, 25°C): $\delta = 139.52$, 133.98, 132.27, 131.54, 128.95, 125.89, 124.37, 123.61, 118.23, 105.29, 97.41, 65.62, 18.86, 11.71 ppm; EI-MS: $m/z$: calcd for $C_{39}H_{52}Si_2O$: 592; found: 592 $[M]^+$.

**General procedure for the preparation of 6b–6d with 6b as a detailed example**

*Compound **6b***: Ester **4** (0.418 g, 1.0 mmol), copper(I) iodide (11.4 mg, 0.060 mmol), dichlorobis(triphenylphosphine)palladium(II) (56 mg, 0.079 mmol) and $Et_3N$ (40 mL) were dissolved in THF (150 mL) in a three-neck flask under nitrogen. The solution was purged with nitrogen for 1 h, followed by the addition of **5b** (1.24 mL, 3 mmol). The mixture was stirred for 20 min before the temperature was raised to 55°C for 24 h. Removal of the solvent afforded a residue that was extracted into $CH_2Cl_2$ (150 mL), washed with $H_2O$ (2×40 mL), and dried over $MgSO_4$. The crude material, obtained after removal of the $CH_2Cl_2$, was purified by means of column chromatography on silica gel by using ethyl acetate/petroleum ether (1:20) as the eluant, to afford a yellow-green solid (0.52 g, 95%). $^1$H NMR (300 MHz, $CDCl_3$, 25°C): $\delta = 8.86$ (s, 2H; $^1$H, $^3$H), 8.67 (d, $J = 9.1$ Hz, 2H; $^5$H, $^9$H), 8.45 (s, 1H; $^7$H), 8.23 (d, $J = 9.1$ Hz, 2H; $^4$H, $^{10}$H), 7.68 (d, $J = 8.4$ Hz, 4H; $^{3B}$H, $^{5B}$H), 7.48 (d, $J = 8.4$ Hz, 4H; $^{2B}$H, $^{6B}$H), 4.09 (s, 3H; OMe), 1.38 ppm (s, 18H; *t*Bu); $^{13}$C NMR (75 MHz, $CDCl_3$, 25°C): $\delta = 167.28$, 152.17, 133.94, 132.11, 131.64, 131.14, 128.89, 128.05, 126.55, 126.27, 125.54, 124.24, 120.46, 118.80, 96.12, 87.11, 52.27, 34.94, 31.26 ppm; EI-MS: $m/z$: calcd for $C_{42}H_{36}O_2$: 572.2715; found: 572.2710 $[M]^+$.

*Compound **6c***: Ester **4** (0.836 g, 2.00 mmol), copper(I) iodide (22.8 mg, 0.120 mmol) dichlorobis(triphenylphosphine)palladium(II) (112 mg, 0.160 mmol), THF (100 mL), $Et_3N$ (40 mL), **5c** (1.07 g, 5 mmol). Column chromatography: silica gel, ethyl acetate/petroleum ether (1:20). Yield:

  

1.25 g, 91%. $^1$H NMR (300 MHz, $CDCl_3$, 25 °C): $\delta$ = 8.89 (s, 2H; $^1$H, $^3$H), 8.74 (d, $J$ = 9.1 Hz, 2H; $^5$H, $^9$H), 8.54 (s, 1H; $^7$H), 8.29 (d, $J$ = 9.1 Hz, 2H; $^4$H, $^{10}$H), 7.58 (d, $J$ = 1.8 Hz, 4H; $^{2B}$H, $^{6B}$H), 7.49 (t, $J$ = 1.8 Hz, 2H; $^{4B}$H), 4.10 (s, 3H; OMe), 1.41 ppm (s, 36H; *t*Bu); $^{13}$C NMR (75 MHz, $CDCl_3$, 25 °C): $\delta$ = 167.39, 151.27, 134.36, 132.24, 131.35, 129.05, 128.18, 126.65, 126.56, 126.08, 124.51, 123.29, 122.43, 119.05, 97.21, 86.37, 52.36, 34.98, 31.45 ppm; EI-MS: *m*/*z*: calcd for $C_{50}H_{52}O_2$: 684.3967; found: 684.3933 $[M]^+$.

*Compound* ***6d***: Ester **4** (1.672 g, 4 mmol), copper(I) iodide (45.6 mg, 0.24 mmol), dichlorobis(triphenylphosphine)palladium(II) (224 mg, 0.32 mmol), THF (150 mL), $Et_3N$ (40 mL), **5d** (2.00 g, 10 mmol). Column chromatography: silica gel, ethyl acetate/petroleum (1:6). Yield: 2.19 g, 87%. $^1$H NMR (300 MHz, $CDCl_3$, 25 °C): $\delta$ = 8.84 (s, 2H; $^1$H, $^3$H), 8.69 (d, $J$ = 9.1 Hz, 2H; $^5$H, $^9$H), 8.39 (s, 1H; $^7$H), 8.22 (d, $J$ = 9.1 Hz, 2H; $^4$H, $^{10}$H), 7.19 (s, 4H; $^{3B}$H, $^{5B}$H), 4.09 (s, 3H; OMe), 2.71 (s, 12H; Me), 1.36 ppm (s, 18H; *t*Bu); $^{13}$C NMR (75 MHz, $CDCl_3$, 25 °C): $\delta$ = 167.37, 151.72, 140.18, 133.88, 131.86, 131.33, 128.98, 128.19, 126.58, 126.48, 124.57, 124.17, 120.25, 119.57, 95.26, 94.18, 52.34, 34.70, 31.29, 21.71 ppm; EI-MS: m/z: calcd for $C_{46}H_{44}O_2$: 628.3341; found: 628.3329 $[M]^+$.

**General procedure for the preparation of 7b–7d with 7b as a detailed example**

*Compound* ***7b***: Ester **6b** (0.35 g, 0.61 mmol) was dissolved in dry $Et_2O$ (150 mL) in a three-neck flask under an atmosphere of nitrogen. To this solution $LiAlH_4$ (34.8 mg, 0.92 mmol) was added slowly and the mixture was stirred for 1 h at RT. The mixture was added to wet ethyl acetate. To this solution, dilute HCl was carefully added. The separated organic phase was washed with $H_2O$ and dried over $MgSO_4$. The residue that remained after filtration and removal of the volatile component, was purified by means of column chromatography by using ethyl acetate/petroleum ether (1:2) as eluant to afford a yellow-green solid (0.31 g, 93%). $^1$H NMR (300 MHz, $CDCl_3$, 25 °C): $\delta$ = 8.65 (dd, $J$ = 1.4 Hz, $J'$ = 9.1 Hz, 2H; $^5$H, $^9$H), 8.39 (d, $J$ = 1.0 Hz, 1H; $^7$H), 8.19 (s, 2H; $^1$H, $^3$H), 8.14 (dd, $J$ = 1.4, 9.1 Hz, 2H; $^4$H, $^{10}$H), 7.68 (d, $J$ = 8.3 Hz, 4H; $^{3B}$H, $^{5B}$H), 7.48 (d, $J$ = 8.3 Hz, 4H; $^{2B}$H, $^{6B}$H), 5.15 (s, 2H; $OCH_2$), 1.31 ppm (s, 18H; *t*Bu); $^{13}$C NMR (75 MHz, $CDCl_3$, 25 °C): $\delta$ = 152.06, 139.44, 133.08, 131.60, 128.63, 125.89, 125.53, 124.55, 124.21, 123.96, 120.56, 118.38, 95.73, 87.40, 65.65, 34.94, 31.27 ppm; EI-MS: m/z: calcd for $C_{41}H_{36}O$: 544.2766; found: 544.2772 $[M]^+$.

*Compound* ***7c***: Ester **6c** (0.85 g, 1.2 mmol), $LiAlH_4$ (70.7 mg, 1.86 mmol), $Et_2O$ (200 mL). Column chromatography: silica gel, ethyl acetate/petroleum ether (1:4). Yield: 0.60 g, 74%. $^1$H NMR (300 MHz, $CDCl_3$, 25 °C): $\delta$ = 8.58 (d, $J$ = 9.1 Hz, 2H; $^5$H, $^9$H), 8.48 (s, 1H; $^7$H), 8.09 (s, 2H; $^1$H, $^3$H), 8.06 (d, $J$ = 9.1 Hz, 2H; $^4$H, $^{10}$H), 7.63 (d, $J$ = 1.8 Hz, 4H; $^{2B}$H, $^{6B}$H), 7.53 (t, $J$ = 1.8 Hz, 2H; $^{4B}$H), 5.11 (s, 2H; $OCH_2$), 1.45 ppm (s, 36H; *t*Bu); $^{13}$C NMR (75 MHz, $CDCl_3$, 25 °C): $\delta$ = 151.20, 139.38, 133.28, 131.56, 131.52, 128.57, 126.04, 125.84, 124.46, 124.11, 123.64, 123.13, 122.58, 118.36, 96.73, 86.72, 65.58, 34.95, 31.45 ppm; EI-MS: *m*/*z* calcd for $C_{49}H_{54}O$: 658 4175; found: 658.4183 $[M]^+$.

*Compound* ***7d***: Ester **6d** (0.20 g, 0.32 mmol), $LiAlH_4$ (18.1 mg, 0.480 mmol), $Et_2O$ (100 mL). Column chromatography: silica gel, ethyl acetate/petroleum ether (1:2). Yield 0.19 g, 99%. $^1$H NMR (300 MHz, $CDCl_3$, 25 °C): $\delta$ = 8.65 (d, $J$ = 9.0 Hz, 2H; $^5$H, $^9$H), 8.34 (s, 1H; $^7$H), 8.17 (s, 2H; $^1$H, $^3$H), 8.14 (d, $J$ = 9.1 Hz, 2H; $^4$H, $^{10}$H), 7.19 (s, 4H; $^{3B}$H, $^{5B}$H), 5.14 (s, 2H; $OCH_2$), 2.71 (s, 12H; Me), 1.36 ppm (s, 18H; *t*Bu); $^{13}$C NMR (75 MHz, $CDCl_3$, 25 °C): $\delta$ = 151.55, 140.12, 139.45, 132.96, 131.71, 131.28, 128.62, 126.01, 124.75, 124.14, 123.93, 120.38, 119.07, 95.58, 93.73,65.67, 34.68, 31.29, 21.73 ppm; EI-MS: *m*/*z* calcd for $C_{45}H_{44}O$: 600.3392; found: 600.3411 $[M]^+$.

**General procedure for the preparation of target compounds with DPP1 as a detailed example**

*Compound* ***DP1***: NaH (0.144 g, 6 mmol) was added to a solution of pyrenyl-2-methanol, **3** (0.696 g, 3 mmol) dissolved in dry THF (50 mL) under nitrogen. The solution was stirred for 1 h at 60 °C and then cooled to RT. α,α′-dibromo-*m*-xylene (0.396 g, 1.5 mmol) was then added to this solution, which was stirred for a further 2 h, and then heated at reflux overnight. The reaction mixture was cooled to RT and poured into ethyl acetate (150 mL), followed by careful addition of $H_2O$ (60 mL). The organic layer was separated, and the aqueous phase was extracted with $CH_2Cl_2$ (3×50 mL). The combined organic phases were washed with $H_2O$ (2×40 mL) and dried over $MgSO_4$. Filtration and removal of the volatile component gave the crude material which was purified by means of column chromatography on silica gel by using ethyl acetate/petroleum ether (1:8) as the eluant to afford a white solid (0.81 g, 95%). $^1$H NMR (300 MHz, $CDCl_3$, 25 °C): $\delta$ = 8.18 (s, 4H; $^1$H, $^3$H), 8.02 (d, $J$ = 7.8 Hz, 4H; $^6$H, $^8$H), 7.99 (s, 8H; $^4$H, $^5$H, $^9$H, $^{10}$H), 7.98 (m, 2H; $^7$H), 7.52 (s, 1H; $^{2P}$H), 7.48 (m, 3H; $^{4P}$H, $^{5P}$H, $^{6P}$H), 5.02 (s, 4H; $OCH_2$Pyr), 4.72 ppm (s, 4H; $PhCH_2O$); $^{13}$C NMR (75 MHz, $CDCl_3$, 25 °C): $\delta$ = 139.05, 136.50, 131.71, 131.54, 128.93, 127.94, 127.68, 127.53, 126.12, 125.33, 125.05, 124.69, 124.50, 73.07, 72.79 ppm; EI-MS: m/z: calcd for $C_{42}H_{30}O_2$: 566; found: 566 $[M]^+$; elemental analysis calcd (%) for $C_{42}H_{30}O_2$: C 89.02, H 5.65; found: C 88.44, H 5.28.

*Compound* ***DP2***: Compound **7a** (1.20 g, 2.02 mmol), $Et_2O$ (500 mL), NaH (0.072 g, 3 mmol), α,α′-dibromo-*m*-xylene (0.275 g, 1.01 mmol), reflux 2 d. Column chromatography: silica gel, $CH_2Cl_2$/petroleum ether (1:4). Yield: 0.68 g, 52%. $^1$H NMR (300 MHz, $CDCl_3$, 25 °C): $\delta$ = 8.59 (d, $J$ = 9.1 Hz, 4H; $^5$H, $^9$H), 8.26 (s, 2H; $^7$H), 8.21 (s, 4H; $^1$H, $^3$H), 8.17 (d, $J$ = 9.1 Hz, 4H; $^4$H, $^{10}$H), 7.52 (s, 1H; $^{2P}$H), 7.43 (s, 3H; $^{4P}$H, $^{5P}$H, $^{6P}$H), 5.02 (s, 4H; $OCH_2$Pyr), 4.74 (s, 4H; $OCH_2Ph$), 1.16–1.15 ppm (m, 84H; Si*i*Pr); $^{13}$C NMR (75 MHz, $CDCl_3$, 25 °C): $\delta$ = 138.69, 137.02, 133.96, 132.29, 131.45, 129.02, 128.70, 127.34, 127.28, 125.83, 125.22, 124.39, 123.68, 118.17, 105.29, 97.31, 72.68, 72.62, 18.86, 11.68 ppm; EI-MS: *m*/*z*: calcd for $C_{86}H_{110}Si_4O_2$: 1286; found: 1286 $[M]^+$; elemental analysis calcd (%) for $C_{86}H_{110}Si_4O_2$: C 80.19, H 8.61; found: C 80.08, H 8.63.

*Compound* ***DP3***: Compound **7b** (0.327 g, 0.6 mmol), NaH (0.056 g, 2 mmol), THF (100 mL), α,α′-dibromo-*m*-xylene (81.6 mg, 0.3 mmol). Column chromatography: silica gel, $CH_2Cl_2$/petroleum ether (1:4). Yield: 0.26 g, 73%. $^1$H NMR (300 MHz, $CDCl_3$, 25 °C): $\delta$ = 8.48 (d, $J$ = 9.1 Hz, 4H; $^5$H, $^9$H), 8.32 (s, 2H; $^7$H), 8.10 (s, 4H; $^1$H, $^3$H), 7.99 (d, $J$ = 9.1 Hz, 4H; $^4$H, $^{10}$H), 7.68 (d, $J$ = 8.4 Hz, 8H; $^{3B}$H, $^{5B}$H), 7.58 (s, 1H; $^{2Ph}$H), 7.48 (d, $J$ = 8.4 Hz, 8H; $^{2B}$H, $^{6B}$H), 7.42 (s, 3H; $^{4P}$H, $^{5P}$H, $^{6P}$H), 4.95 (s, 4H; $OCH_2$Pyr), 4.74 (s, 4H; $OCH_2Ph$), 1.39 ppm (s, 36H; *t*Bu); $^{13}$C NMR (75 MHz, $CDCl_3$, 25 °C): $\delta$ = 151.90, 138.79, 136.86, 132.99, 131.60, 131.55, 131.40, 128.62, 128.57, 127.21, 127.16, 125.68, 125.48, 124.99, 124.40, 123.66, 120.64, 118.20, 95.62, 87.51, 72.66, 72.57, 34.89, 31.26 ppm; EI-MS: *m*/*z*: calcd for $C_{90}H_{78}O_2$: 1191.6; found: 1192 $[M]^+$; elemental analysis calcd (%) for $C_{90}H_{78}O_2$: C 90.72, H 6.60; found: C 91.49, H 6.70.

*Compound* ***DP4***: Compound **7c** (0.74 g, 1.13 mmol), THF (150 mL), NaH (0.10 g, 4.2 mmol), α,α′-dibromo-*m*-xylene (0.139 g, 0.512 mmol). Column chromatography: silica gel, $CH_2Cl_2$/petroleum ether (1:4). Yield: 0.40 g, 54%. $^1$H NMR (300 MHz, $CDCl_3$, 25 °C): $\delta$ = 8.69 (d, $J$ = 9.1 Hz, 4H; $^5$H, $^9$H), 8.49 (s, 2H; $^7$H), 8.25 (s, 4H; $^1$H, $^3$H), 8.21 (d, $J$ = 9.1 Hz, 4H; $^4$H, $^{10}$H), 7.49 (d, $J$ = 1.8 Hz, 8H; $^{2B}$H, $^{6B}$H), 7.49 (t, $J$ = 1.8 Hz, 4H; $^{4B}$H), 7.46 (s, 1H, $^{2P}$H), 7.44 (d, $J$ = 1.9 Hz, 3H; $^{B}$H), 5.04 (s, 4H; $OCH_2$Pyr), 4.76 (s, 4H; $OCH_2Ph$), 1.41 ppm (s, 72H; *t*Bu); $^{13}$C NMR (75 MHz, $CDCl_3$, 25 °C): $\delta$ = 151.19, 138.72, 136.98, 133.40, 131.68, 131,61, 128.73, 127.37, 127.28, 126.06, 125.99, 125.14, 124.66, 123.91, 123.11, 122.60, 121.21, 118.46, 96.72, 86.73, 72.68, 65.76, 34.96, 31.57 ppm; EI-MS: *m*/*z*: calcd for $C_{106}H_{110}O_2$: 1416.0; found: 1420 $[M]^+$; elemental analysis calcd (%) for $C_{106}H_{110}O_2$: C 89.91, H, 7.83; found: C 89.89, H 8.13.

*Compound* ***DP5***: Compound **7d** (0.50 g, 0.83 mmol), THF (150 mL), NaH (0.072 g, 3 mmol) α,α′-dibromo-*m*-xylene (0.113 g, 0.416 mmol). Column chromatography: silica gel, $CH_2Cl_2$/petroleum ether (1:4). Yield: 0.42 g, 77%. $^1$H NMR (300 MHz, $CDCl_3$, 25 °C): $\delta$ = 8.59 (d, $J$ = 9.0 Hz, 4H; $^5$H, $^9$H), 8.31 (s, 2H; $^7$H), 8.16 (s, 4H, $^1$H, $^3$H), 7.08 (d, $J$ = 9.1 Hz, 2H; $^4$H, $^{10}$H), 7.59 (s, 1H; $^{2P}$H), 7.43 (s, 3H; $^{4P}$H, $^{5P}$H, $^{6P}$H), 7.18 (s, 8H; $^{3B}$H, $^{5B}$H), 5.00 (s, 4H; $OCH_2$Pyr), 4.77 (s, 4H; $OCH_2Ph$), 2.68 (s, 24H; Me), 1.37 ppm (s, 36H; *t*Bu); $^{13}$C NMR (75 MHz, $CDCl_3$, 25 °C): $\delta$ = 151.47, 140.91, 138.77, 136.93, 132.92, 131.56, 131.25, 128.68, 128.61, 127.30, 127.24, 125.88, 125.04, 124.66, 124.10, 123.89, 120.44, 118.98, 95.67, 93.67, 72.66, 72.61, 34.67, 31.30, 27.71 ppm; EI-MS: *m*/*z*: calcd for $C_{98}H_{94}O_2$: 1303.8; found: 1304 $[M]^+$; elemental analysis calcd (%) for $C_{98}H_{94}O_2$: C 90.28, H 7.27; found: C 90.19, H 7.31.

  

## Acknowledgements

We thank EPSRC (EP/D001194) and Newcastle University for financial support of this work. The EPSRC-sponsored Mass Spectrometry Service at Swansea is thanked for recording the mass spectra.

[1] a) J. M. Lehn, *Angew. Chem.* **1988**, *100*, 91–116; *Angew. Chem. Int. Ed. Engl.* **1988**, *27*, 89–112; b) C. A. Hunter, K. R. Lawson, J. Perkins, C. J. Urch, *J. Chem. Soc., Perkin Trans. 2* **2001**, 651–669.

[2] a) F. M. Raymo, J. F. Stoddart, *Chem. Rev.* **1999**, *99*, 1643–1663; b) C. G. Claessens, J. F. Stoddart, *J. Phys. Org. Chem.* **1997**, *10*, 254–272; c) J. L. Lindsey, *New J. Chem.* **1991**, *15*, 153–180; d) L. F. Lindoy, I. M. Atkinson, in *Self-Assembly in Supramolecular Systems* (Ed.: J. F. Stoddart) RSC, Cambridge, **2000**.

[3] a) E. Gazit, *FASEB J.* **2002**, *16*, 77–83; b) F. Bathe, K. Hahlen, R. Dombi, L. Driller, M. Schliwa, G. Woehkle, *Mol. Biol. Cell* **2005**, *16*, 3529–3537.

[4] A. L. Ringer, M. O. Sinnokrot, R. P. Lively, C. D. Sherrill, *Chem. Eur. J.* **2006**, *12*, 3821–3828.

[5] C. A. Hunter, J. K. M. Sanders, *J. Am. Chem. Soc.* **1990**, *112*, 5525–5534.

[6] S. Aravinda, N. Shamala, C. Das, A. Sriranjini, I. L. Karle, P. Balaram, *J. Am. Chem. Soc.* **2003**, *125*, 5308–5315.

[7] a) F. Cozzi, M. Cinquini, R. Annuziata, T. Dwyer, J. S. Siegel, *J. Am. Chem. Soc.* **1992**, *114*, 5729–5733; b) F. Cozzi, M. Cinquini, R. Annunziata, J. S. Siegel, *J. Am. Chem. Soc.* **1993**, *115*, 5330–5331; c) R. Laatikainen, J. Ratilainen, R. Sebastian, H. Santa, *J. Am. Chem. Soc.* **1995**, *117*, 11006–11010.

[8] a) T. Sato, T. Tsuneda, K. Hirao, *J. Chem. Phys.* **2005**, *123*, 104307; b) G. Raviishanker, D. L. Beveridge, *J. Am. Chem. Soc.* **1985**, *107*, 2565–2566; c) W. L. Jorgensen, D. L. Serenance, *J. Am. Chem. Soc.* **1990**, *112*, 4768–4777.

[9] A. Harriman, *Angew. Chem.* **1999**, *111*, 996–1000; *Angew. Chem. Int. Ed.* **1999**, *38*, 945–949.

[10] D. E. Janzen, M. W. Burand, P. C. Ewbank, T. M. Pappenfus, H. Higuchi, D. A. da Silva, V. G. Young, J. L. Bredas, K. R. Mann, *J. Am. Chem. Soc.* **2004**, *126*, 15295–15308.

[11] J. Zyss, I. Ledoux, S. Volkov, V. Chernyak, S. Mukamel, G. P. Bartholomew, G. C. Bazan, *J. Am. Chem. Soc.* **2000**, *122*, 11956–11962.

[12] C. J. Yang, S. Jockusch, M. Vicens, N. J. Turro, W. Tan, *PNAS* **2005**, *102*, 17278–17283.

[13] J. Pina, S. Seixas de Melo, F. Pina, C. Lodeiro, J. C. Lima, A. Jorge Parola, *Inorg. Chem.* **2005**, *44*, 7449–7458.

[14] S. Y. Moon, N. J. Youn, S. M. Park, S.-K. Chang, *J. Org. Chem.* **2005**, *70*, 2394–2397.

[15] M. T. Albelda, E. García-España, L. Gil, J. C. Lima, C. Lodeiro, J. Seixas de Melo, A. J. Parola, F. Pina, C. Soriano, *J. Phys. Chem. B* **2003**, *107*, 6573–6578.

[16] J. B. Birks, D. J. Dyson, I. H. Munro, *Proc. R. Soc. London, Ser A* **1963**, *275*, 575–588.

[17] a) B. Shazmann, N. Alhashimy, D. Diamond, *J. Am. Chem. Soc.* **2006**, *128*, 8607–8614; b) S. H. Kim, J. S. Kim, S. M. Park, S.-K. Chang, *Org. Lett.* **2006**, *8*, 371–374; c) X. Xiao, W. Xu, D. Zhang, H. Xu, L. Liu, D. Zhu, *New J. Chem.* **2005**, *29*, 1291–1294; d) H. Yuasa, N. Miyagawa, T. Izumi, M. Nakatani, M. Izumi, H. Hashimoto, *Org. Lett.* **2004**, *6*, 1489–1492; e) H. Yuasa, N. Miyagawa, M. Nakatani, M. Izumi, H. Hashimoto, *Org. Biomol. Chem.* **2004**, *2*, 3548–3556.

[18] J. Duhamel, S. Kanagalingam, T. J. O'Brien, M. W. Ingratta, *J. Am. Chem. Soc.* **2003**, *125*, 12810–12822.

[19] C. R. Ray, J. S. Moore, *Adv. Polym. Sci.* **2005**, *177*, 91–149.

[20] a) A. Ojida, K. Honda, D. Shinmi, S. Kiyonaka, Y. Mori, I. Hamachi, *J. Am. Chem. Soc.* **2006**, *128*, 10452–10459; b) H. Takakusa, K. Kihuchi, Y. Urano, H. Kojima, T. Nagano, *Chem. Eur. J.* **2003**, *9*, 1479; c) P. Jiang, Z. Guo, *Coord. Chem. Rev.* **2004**, *248*, 205–229.

[21] a) K. Fujimoto, Y. Muto, M. Inouye, *Chem. Commun.* **2005**, 4780–4782; b) Z. Wang, D. Zhang, D. Zhu, *Anal. Chim. Acta* **2005**, *549*, 10–13; c) H. K. Cho, D. H. Lee, J. I. Hong, *Chem. Commun.* **2005**, 1690–1692; d) A. Okamoto, Y. Ochi, I. Saito, *Chem. Commun.* **2005**, 1128–1130; e) A. C. Benniston, A. Harriman, D. J. Lawrie, A. Mayeux, K. Rafferty, O. D. Russell, *Dalton Trans.* **2003**, 4762–4769; f) K. Yamana, Y. Ohtani, H. Nakano, I. Saito, *Bioorg. Med. Chem. Lett.* **2003**, *13*, 3429–3431; g) R.-H. Yang, W.-H. Chan, A. W. M. Lee, P.-F. Xia, H-K. Zhang, K. Li, *J. Am. Chem. Soc.* **2003**, *125*, 2884–2885; h) J. S. Kim, O. J. Shon, J. A. Rim, S. K. Kim, J. Yoon, *J. Org. Chem.* **2002**, *67*, 2348–2351.

[22] J. B. Birks, *Photophysics of Aromatic Molecules*, Wiley Interscience, London, **1970**.

[23] A. Harriman, M. Hissler, R. Ziessel, *Phys. Chem. Chem. Phys.* **1999**, *1*, 4203–4211.

[24] D. V. O'Connor, D. Phillips, *Time-Correlated Single-Photon Counting*, API, US, **1986**.

[25] a) N. J. Turro, M. Aikawa, A. Yekta, *J. Am. Chem. Soc.* **1979**, *101*, 772–774; b) M. K. Sonnenschein, R. G. Weiss, *J. Phys. Chem.* **1988**, *92*, 6828–6835; c) E. A. Chandross, C. J. Dempster, *J. Am. Chem. Soc.* **1970**, *92*, 3586–3593; d) K. Hara, H. Yano, *J. Am. Chem. Soc.* **1988**, *110*, 1911–1915; e) W. Rettig, B. Paeplow, H. Herbst, K. Müllen, J.-P. Desvergne, H. Bouas-Laurent, *New J. Chem.* **1999**, *23*, 453–460.

[26] A. Bondi, *J. Phys. Chem.* **1964**, *68*, 441–451.

[27] a) A. C. Benniston, A. Harriman, D. J. Lawrie, S. A. Rostron, *Eur. J. Org. Chem.* **2004**, *10*, 2272–2276; b) R. Ziessel, C. Goze, G. Ulrich, M. Césario, P. Retailleau, A. Harriman, J. P. Rostron, *Chem. Eur. J.* **2005**, *11*, 7366–7378; c) S.-W. Yang, A. Elangovan, K.-C. Hwang, T.-I. Ho, *J. Phys. Chem. B* **2005**, *109*, 16628–16635.

[28] G. Porter, M. R. Topp, *Proc. R. Soc. London, Ser A* **1970**, *315*, 163–184.

[29] J. T. Richards, G. West, J. K. Thomas, *J. Phys. Chem.* **1970**, *74*, 4137–4141.

[30] S. P. McGlynn, T. Azumi, M. Kinoshita, *Molecular Spectroscopy of the Triplet State*, Prentice-Hall, New Jersey, **1969**.

[31] S. Watanabe, A. Furube, R. Katoh, *J. Phys. Chem. A* **2006**, *110*, 10173–10178.

[32] S. Samori, S. Tojo, M. Fujitsuka, S. W. Yang, T. I. Ho, J. S. Yang, T. Majima, *J. Phys. Chem. B* **2006**, *110*, 13296–13303.

[33] S. K. Lower, M. A. El-Sayed, *Chem. Rev.* **1966**, *66*, 199–241.

[34] J. Saltiel, G. R. Marchand, W. K. Smothers, S. A. Stout, J. L. Charlton, *J. Am. Chem. Soc.* **1981**, *103*, 7159–7164.

[35] J. L. Charlton, R. Dabestani, J. Saltiel, *J. Am. Chem. Soc.* **1983**, *105*, 3473–3476.

[36] D. D. Perrin, W. L. F. Armarego, *Purification of Laboratory Chemicals*, 3rd ed., Pergamon Press, Oxford, **1988**.

[37] H. Vollmann, H. Becker, M. Correll, H. Streek, *J. Liebigs Ann. Chem.* **1937**, *531*, pp 1–5.

[38] J. A. John, J. M. Tour, *Tetrahedron* **1997**, *53*, 15515–15534.

[39] Y. Pan, Z. Peng, J. S. Melinger, *Tetrahedron* **2003**, *59*, 5495–5506.

[40] M. T. Tirpak, C. A. Hollingsworth, J. H. Wotiz, *J. Org. Chem.* **1960**, *25*, 687–690.

[41] S. L. Murov, I. Carmichael, G. L. Hug, *Handbook of Photochemistry*, 2nd ed., Marcel-Dekker, New York, **1993**.

Received: October 20, 2006
Published online: February 7, 2007

  